Steel Wool for Water Treatment: Intrinsic Reactivity and Defluoridation Efficiency

Authors:

Benjamin Hildebrant, Arnaud Igor Ndé-Tchoupé, Mesia Lufingo, Tobias Licha, Chicgoua Noubactep

Date Submitted: 2020-05-02

Keywords: zero-valent iron, water defluoridation, intrinsic reactivity, ethylenediaminetetraacetic acid, dye discoloration

Abstract:

Studies were undertaken to characterize the intrinsic reactivity of Fe0-bearing steel wool (Fe0 SW) materials using the ethylenediaminetetraacetate method (EDTA test). A 2 mM Na2-EDTA solution was used in batch and column leaching experiments. A total of 15 Fe0 SW specimens and one granular iron (GI) were tested in batch experiments. Column experiments were performed with four Fe0 SW of the same grade but from various suppliers and the GI. The conventional EDTA test (0.100 g Fe0, 50 mL EDTA, 96 h) protocol was modified in two manners: (i) Decreasing the experimental duration (down to 24 h) and (ii) decreasing the Fe0 mass (down to 0.01 g). Column leaching studies involved glass columns filled to 1/4 with sand, on top of which 0.50 g of Fe0 was placed. Columns were daily gravity fed with EDTA and effluent analyzed for Fe concentration. Selected reactive Fe0 SW specimens were additionally investigated for discoloration efficiency of methylene blue (MB) in shaken batch experiments (75 rpm) for two and eight weeks. The last series of experiments tested six selected Fe0 SW for water defluoridation in Fe0/sand columns. Results showed that (i) the modifications of the conventional EDTA test enabled a better characterization of Fe0 SW; (ii) after 53 leaching events the Fe0 SW showing the best kEDTA value released the lowest amount of iron; (iii) all Fe0 specimens were efficient at discoloring cationic MB after eight weeks; (iv) limited water defluoridation by all six Fe0 SW was documented. Fluoride removal in the column systems appears to be a viable tool to characterize the Fe0 long-term corrosion kinetics. Further research should include correlation of the intrinsic reactivity of SW specimens with their efficiency at removing different contaminants in water.

Record Type: Published Article

Submitted To: LAPSE (Living Archive for Process Systems Engineering)

Citation (overall record, always the latest version):	LAPSE:2020.0410
Citation (this specific file, latest version):	LAPSE:2020.0410-1
Citation (this specific file, this version):	LAPSE:2020.0410-1v1

DOI of Published Version: https://doi.org/10.3390/pr8030265

processes

MDPI

Article

Steel Wool for Water Treatment: Intrinsic Reactivity and Defluoridation Efficiency

Benjamin Hildebrant [1], Arnaud Igor Ndé-Tchoupé [2], Mesia Lufingo [3], Tobias Licha [4] and Chicgoua Noubactep [1,5,*]

1 Angewandte Geologie, Universität Göttingen, Goldschmidtstraße 3, D-37077 Göttingen, Germany; hildebrantb@gmail.com
2 Department of Chemistry, Faculty of Sciences, University of Douala, Douala B.P. 24157, Cameroon; ndetchoupe@gmail.com
3 Department of Water and Environmental Science and Engineering, Nelson Mandela African Institution of Science and Technology, Arusha P.O. Box 447, Tanzania; lufingom@nm-aist.ac.tz
4 Institut für Geologie, Mineralogie und Geophysik Fakultät für Geowissenschaften Ruhr-Universität Bochum Universitätsstraße, 15044801 Bochum, Germany; tobias.licha@rub.de
5 School of Earth Science and Engineering, Hohai University, Fo Cheng Xi Road 8, Nanjing 211100, China
* Correspondence: cnoubac@gwdg.de

Received: 31 December 2019; Accepted: 24 February 2020; Published: 26 February 2020

Abstract: Studies were undertaken to characterize the intrinsic reactivity of Fe^0-bearing steel wool (Fe^0 SW) materials using the ethylenediaminetetraacetate method (EDTA test). A 2 mM Na_2-EDTA solution was used in batch and column leaching experiments. A total of 15 Fe^0 SW specimens and one granular iron (GI) were tested in batch experiments. Column experiments were performed with four Fe^0 SW of the same grade but from various suppliers and the GI. The conventional EDTA test (0.100 g Fe^0, 50 mL EDTA, 96 h) protocol was modified in two manners: (i) Decreasing the experimental duration (down to 24 h) and (ii) decreasing the Fe^0 mass (down to 0.01 g). Column leaching studies involved glass columns filled to 1/4 with sand, on top of which 0.50 g of Fe^0 was placed. Columns were daily gravity fed with EDTA and effluent analyzed for Fe concentration. Selected reactive Fe^0 SW specimens were additionally investigated for discoloration efficiency of methylene blue (MB) in shaken batch experiments (75 rpm) for two and eight weeks. The last series of experiments tested six selected Fe^0 SW for water defluoridation in Fe^0/sand columns. Results showed that (i) the modifications of the conventional EDTA test enabled a better characterization of Fe^0 SW; (ii) after 53 leaching events the Fe^0 SW showing the best k_{EDTA} value released the lowest amount of iron; (iii) all Fe^0 specimens were efficient at discoloring cationic MB after eight weeks; (iv) limited water defluoridation by all six Fe^0 SW was documented. Fluoride removal in the column systems appears to be a viable tool to characterize the Fe^0 long-term corrosion kinetics. Further research should include correlation of the intrinsic reactivity of SW specimens with their efficiency at removing different contaminants in water.

Keywords: dye discoloration; ethylenediaminetetraacetic acid; intrinsic reactivity; water defluoridation; zero-valent iron

1. Introduction

The knowledge that metallic iron (Fe^0) is the parent of iron oxides and hydroxides ("rust", iron corrosion products or FeCPs) is well-established and has been used for water treatment for more than 170 years [1–7]. As a rule, small pieces of Fe^0 (iron filings, iron shaving, scrap iron, steel wool) are brought in contact with polluted water in static [8], semi-dynamic [2], or dynamic [6] systems. A myriad of Fe^0 materials have been manufactured or selected, tested, and used for water

treatment both at small and large scales between 1850 and 1930 [1,9–11]. By the early 20th century, around World War I, steel wool (SW) has been mass-produced, and became an essential cleaning instrument in households. This mass-production makes SW probably the most widespread Fe^0 materials worldwide [12–14]. In particular, each visually thin strand of SW is made of thousands of metal fibres that are very reactive [15,16]. The rapid kinetics of SW corrosion justifies its use in scholar practical demonstrations [17–20].

The first application of SW for safe drinking water provision is probably the one presented by Emmons in the 1950s—Emmons Process [21,22]. After the Emmons Process, Fe^0 SW and other forms of Fe^0 materials were intermittently reported in water treatment worldwide [15,23–27]. In the western scientific literature, Fe^0 was rediscovered in the 1980s [16,25,28]. For example, Tseng et al. [25] used SW to concentrate radioactive Cobalt in sea water samples; Erickson et al. [29–31] used SW to reinforce the phosphorus removal capacity of filtration systems; Albinsson et al. [26] and Del Cul and Bostick [32,33] used SW to mitigate the migration of radionuclides from waste repositories; James et al. [34] used SW to reinforce the phosphorus removal capacity of peat based filtration systems. In general, testing SW for water treatment became common place, even though available results are to be regarded as independent reports [35]. From 1995 on, SW was tested for the removal of various contaminants including arsenic [36,37], chromium [38,39], nitrate [40,41], pathogens [42,43], and selenium [44]. However, SW is just used as a class of reactive material mostly without any reactivity characterization [35]. To the best of the author's knowledge, Hildebrant [45], Lufingo [14], and Ndé-Tchoupé [13] have presented the first attempts to systematically characterize the intrinsic reactivity of Fe^0 SW.

The named authors basically used the ethylenediaminetetraacetate method (EDTA test) and the methylene blue discoloration method (MB test) [13,14,45]. Lufingo [14] additionally presented a novel test in which EDTA is replaced by 1,10-Phenanthroline (Phen test) [12]. The EDTA and the Phen tests are rooted on the evidence, that the initial Fe^0 dissolution in aqueous solutions containing a complexing agent (EDTA or Phen) is a linear function of time and the slope of the line is characteristic for each Fe^0 specimen. On the other hand, the MB test relies on the evidence that MB adsorption onto positively charged iron corrosion products (FeCPs) is not favorable [46–48]. Accordingly, the kinetics of MB discoloration by Fe^0 materials is slow and can be better characterized [49]. When a Fe^0/sand system is characterized using the MB test, for a certain time frame, the more efficient system is the one depicting the lowest MB discoloration. This observation is justified by the fact that sand, which is an excellent adsorbent for cationic MB is progressively coated by positively charged FeCPs. Coated sand depicts a lower adsorptive affinity for MB than clean sand [46,48]. The merit of the three named tests (EDTA, MB, and Phen) is that, similar to H_2 evolution [50,51], they do characterize an intrinsic property of each Fe^0 (intrinsic reactivity) and results are transferable to all systems, unlike characterization tools based on the Fe^0 removal efficiency for individual contaminants [52–55].

A constant problem within the "Fe^0 remediation" research community is that the terms "efficiency" and "reactivity" are mostly randomly interchanged [49,56–58]. In essence, reactivity is an intrinsic property of a material that cannot change. It can also not be quantified into which number. It can only be indirectly assessed, for example with the dissolution rate in EDTA or Phen solutions. The extent of MB discoloration by a given Fe^0 mass under well-defined conditions can also be used to assess its intrinsic reactivity. In all the cases, unified standard protocols are needed. The Phen test is the current best candidate for such a protocol [12]. Efficiency, on the other hand, is the expression of the reactivity as influenced by operational or site-specific conditions (e.g., pH value, salinity) [57].

The present work is an attempt to correlate "efficiency" and "reactivity" of selected Fe^0 SW by using materials of known intrinsic reactivity (EDTA test) for MB discoloration and water defluoridation. Parallel batch and column experiments are performed and the results are comparatively discussed.

2. Material and Methods

2.1. Aqueous Solutions

2.1.1. EDTA

The ethylenediaminetetraacetic acid (EDTA) solution used for the experiments was prepared by dissolving an analytical grade disodium salt of EDTA (Na_2–EDTA from Merck—Darmstadt/Germany) in tap water and diluting to a concentration of 0.002 M (2 mM). The tap water of the city of Göttingen has a very constant composition with low level of cations. For similar experiments in Cameroon or Tanzania our research group used deionized water.

2.1.2. TISAB

Total ionic strength adjustment buffer (TISAB) was used to regulate the ionic strength and pH of samples prior to determination of fluoride concentration with the ion selective electrode. The buffer solution was prepared by adding 1500 mL of tap water to a 2500 mL glass beaker, to which 114.0 mL of glacial acetic acid, 116.0 g of table salt (NaCl), and 6.42 g of Na_2-EDTA were added. The mixture was heated and stirred with a magnetic stir rod and then allowed to cool to room temperature. Additional tap water was then added until the total solution volume reached 2000 mL, and the pH was adjusted by using a 5 M NaOH solution until a pH value of 5.3 was obtained. The TISAB solution was stored in clean polyethylene bottles.

2.1.3. Methylene Blue ($C_{16}H_{18}ClN_3S$)

Analytical grade Methylene Blue was purchased from Acros Organics and used as received. The working solution had a concentration of 10.0 mg/L. MB is a cationic dye that has a strong affinity for the surface of negatively charged solids [46,59]. MB has a maximum light absorption wavelength of 664.5 nm and a molecular mass of 319.85 g mol^{-1}.

2.1.4. Additional Solutions

A standard iron solution (1000 mg L^{-1}) from Baker JT® was used to calibrate the spectrophotometer. In preparation for spectrophotometric analysis ascorbic acid was used to reduce Fe^{III}-EDTA in solution to Fe^{II}-EDTA. 1,10 orthophenanthroline (ACROS Organics) was used as reagent for Fe^{II} complexation prior to spectrophotometric determination. Other chemicals used in this study included L(+)-ascorbic acid, L-ascorbic acid sodium salt, and sodium acetate. All chemicals were of analytical grade.

2.2. Solid Materials

2.2.1. Sand

The sand used in all of the column experiments is commercially available for aviculture ("Aquarienkies" sand from Quarzverpackungwerek Rosnerski Königslutter/Germany). The grain sizes of used Aquarienkies sand ranged between 2.0 and 4.0 mm (average diameter). The sand was used without additional pretreatment or characterization. Sand was used because of its worldwide availability and its use as admixing agent in Fe^0/H_2O systems [60].

2.2.2. Steel Wool (Fe^0)

A total of fifteen different types of steel wool were used in this work. Six varieties of SW were purchased at a local hardware store in Göttingen (Germany) and two steel wool varieties were purchased in Tengeru (Tanzania). Four of the SW specimens from Germany were from the trademark brand RASKO, consisting of grades 00, 0, 1, 2. The other two German SW varieties were a stainless steel Topfreiniger and a variety from the trademark brand Bobby Mat. The Bobby Mat variety was a fine grade, while the grade of the stainless steel Topfreiniger was not specified, but is herein classified as

coarse grade. The two SW purchased in Tengenru (produced in Kenya) included Champion and Sokoni trademark brands, both being of a fine grade. Five of the SW were purchased in Douala (Cameroon): Trademark brand Grand Menage extra fine and fine SW, trademark brand Socapine very fine SW, Magic Mamy trademark brand coarse SW, and a generic coarse SW. Additional two specimens were produced in China: Trademark brands Suprawisch fine grade SW and Lijia medium grade SW. The specifications of the SW specimens are summarized in Table 1. Apart from chopping the SW samples into pieces of 1–2 cm in length, all materials were used for the experiment in an 'as received' state.

Table 1. Overview of the fifteen different steel wool (SW) specimens used in the experiments. The SW vary from extra fine to coarse grade, and come from Germany, Kenya, Cameroon, and China. Information about SW thickness was deduced from the grade or given by the suppliers.

Material Code	Size	Grade	Thickness (μm)	Trade Name
SW1	fine	00	40	RASKO (Germany)
SW2	medium	0	50	RASKO (Germany)
SW3	medium	1	60	RASKO (Germany)
SW4	medium	2	75	RASKO (Germany)
SW5	fine	00	40	Champion (Kenya)
SW6	fine	00	40	SOKONI (Kenya)
SW7	fine	00	40	BOBBY MAT (Germany)
SW8	coarse	2	75	Stainless steel Topfreiniger (Germany)
SW9	fine	00	40	SOCAPINE (Cameroon)
SW10	extra fine	000	35	Grand Menage (Cameroon)
SW11	fine	0	50	Stainless steel SUPRAWISCH (China)
SW12	medium	1	60	LIJIA (China)
SW13	fine	0	50	Grand Menage (Cameroon)
SW14	coarse	2	75	MAGIC MAMY (Cameroon)
SW15	coarse	3	90	Generic steel wool (Cameroon)

2.3. Experimental Procedure

2.3.1. Iron Dissolution in EDTA

Batch Experiments

Two series of quiescent batch experiments were conducted at room temperature (22 ± 2 °C) in glass beakers and out of direct sunlight:

Experiment 1: The objective was to achieve the best possible linearity of the function [Fe] = f(t). A 0.01 g sample of each steel wool (SW1–SW8) was weighed out and placed in 50 mL of 2 mM EDTA solution. At prefixed intervals, 1 mL samples were taken from each of the beakers and analyzed for Fe.

Experiment 2: Triplicates of each of the following samples placed in beakers containing 50 mL of 2 mM EDTA solution: 0.01 g samples of SW1, SW5, SW9, and granular iron, in addition to a 0.1 g sample of granular iron. The average value of the corresponding triplicates was used for the discussion.

Column Experiments

Five glass columns were filled with 10 cm of sand, on top of which 0.500 grams of Fe^0 material was placed. Each column contained one of the five types of Fe^0 materials being tested. Four steel wool specimens (SW1, SW5, SW6, SW7) and the granular iron (GI) were selected and used. The columns

were then intermittently charged with a gravity driven 2 mM EDTA solution and allowed to set for at least 24 h. About 300 mL of EDTA was added for each leaching event.

The EDTA solution from each column was then drained and collected in a glass cylinder 3–5 times per week. The collected volume was measured and recorded for each leaching event. An amount of 0.5 to 2.0 mL of the effluent solution was taken, extended to 10 mL, and used for Fe determination. After each column was drained of EDTA solution it was refilled with newly prepared solution and the procedure was repeated. The experiment was performed at room temperature (22 ± 2 °C).

2.3.2. Methylene Blue (MB) Discoloration

These experiments involved eight Fe^0 SW (SW1 through SW8) and one GI, involving 10 different systems in triplicates. A total of 30 systems were characterized. Each system consisted of 0.00 or 0.05 g of the Fe^0 specimen (one blank, one GI, and 8 SW), and 22 mL of MB. The initial MB concentration was 10 mg L^{-1}. The 30 systems were placed in test tubes and were allowed to equilibrate on a rotary shaker at 75 rotations per min (rpm) for two or eight weeks. At the end of the equilibration, samples were then analyzed for MB concentration.

2.3.3. Fluoride Removal

Batch Experiments

Nine Fe^0 specimens (SW1–SW8 and GI) were tested for fluoride removal under quiescent conditions for eight weeks. A triplicate set without Fe^0 served as the reference system. Experiments were performed in triplicates. A total of 30 systems were tested. Test tubes were filled with a 25 mg L^{-1} fluoride solution. The average removal value of each sample triplicate was determined and used for the discussion.

Column Experiments

Five glass columns were filled with multiple layers of sand and sand/steel wool mixtures. An amount of 200 mL of sand was poured into the bottom of each column. To assure that the sand was optimally compacted the columns were gently tapped with a 100 mL PET flacon containing water. The reactive zone was placed on top of the sand layer. This reactive zone consisted of a total of 2.0 grams of steel wool mixed with 100 mL of sand. The investigated steel wool specimens were SW1, SW2, SW3, SW4, and SW6 (Table 2). The SW was cut into small pieces (1–2 cm) so that layers of sand could be interspersed between layers of steel wool. On top of the reactive layer, an additional 100 mL of sand was added (Figure 1).

Table 2. The selected metallic iron (Fe^0) SW specimens for investigation in column studies with 25 mg L^{-1} fluoride solution. An amount of 2.0 g of each sample was cut into small pieces and placed in the reactive zone of its respective column.

	Column 1	Column 2	Column 3	Column 4	Column 5
Steel Wool	SW 1	SW 2	SW 3	SW 4	SW 6
Mass (g)	1.985	1.989	2.006	2.009	1.996

The columns were then charged with a gravity driven water solution containing 25 mg L^{-1} of fluoride (about 300 mL). An amount of 15 mL of effluent from each column was collected in plastic sampling containers, after the fluoride solution had been in contact with the steel wool and sand filter for at least 24 h. These effluent samples were used to determine the fluoride concentration, therefore only plastic containers, not glass, could be used. An additional 10 mL water sample from each column was collected in a glass test tube in order to determine iron concentration. The pH of the effluent was

also determined and its total volume recorded. Each time after samples were taken for iron, fluoride, and pH determination, the columns were refilled with freshly prepared fluoride solution.

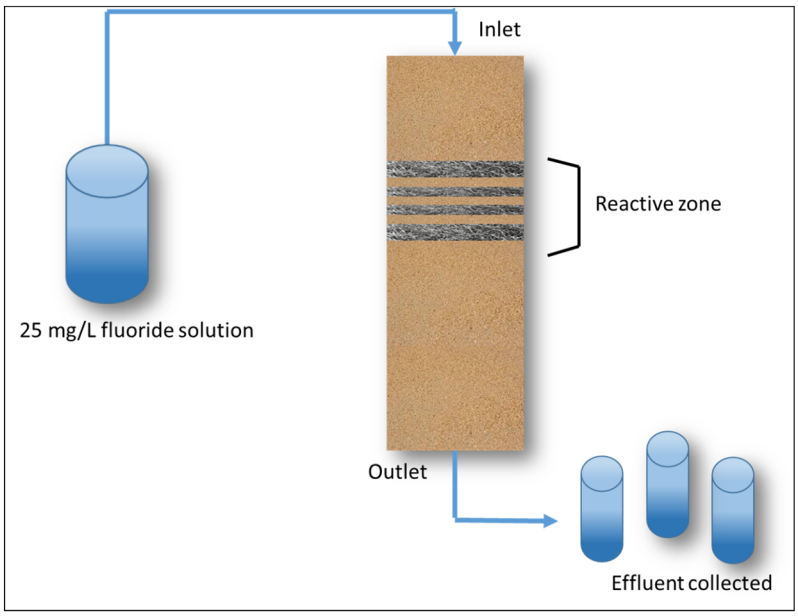

Figure 1. Graphic representation of the experimental setup of the fluoride removal experiment.

2.4. Analytical Methods

2.4.1. UV-Vis Spectrophotometry

A Cary 50 Varian UV-Vis spectrophotometer was used to determine MB and total dissolved iron concentration of the samples. The wavelength was set to 510 and 664.5 nm for dissolved iron and MB, respectively. Determination of dissolved iron followed the 1,10 orthopenanthroline method [61]. Iron samples were prepared by combining: 10 mL of sample + 1 mL ascorbic acid + 8 mL H_2O + 1 mL 1,10-orthophenanthroline.

The UV-Vis spectrophotometer was calibrated for dissolved iron and MB using standard solutions of known concentrations. For iron determination, standard solutions of 0, 2, 4, 6, 8, and 10 mg L^{-1} were prepared from a commercial iron standard solution. Calibration for MB was performed by using standard solutions of 0, 2.5, 5.0, 7.5, and 10 mg L^{-1}.

2.4.2. pH Meter

The pH value of samples were measured with combined gas electrodes (WTW Co., Germany) which were calibrated with five standard solutions of known pH value in accordance with IUPAC recommendations [62]. A magnetic stir bar was placed in the beaker of each of the samples in order to homogenize the solution and prevent statistical error. The electrode measured the pH of each sample for at least 2 min before the data was recorded.

2.4.3. Fluoride Electrode

An ion selective electrode was used for the determination of fluoride from column effluents. A calibration curve was made by recording the potential values for the corresponding fluoride solutions of ten different concentrations: 0.00, 1.25, 2.50, 5.00, 7.50, 10.00, 15.00, 20.00, 25.00, and 30.00 mg L^{-1}. Total ionic strength adjustment buffer with a pH of 5.3 was used with fluoride solutions to reduce the interference of other ions (including OH^- and Fe^{3+}). The measured fluoride potentials were used to calculate fluoride concentrations.

2.5. Expression of Experimental Results

2.5.1. Kinetics of Fe^0 Oxidative Dissolution (k_{EDTA} Value)

The initial rate of iron dissolution from each Fe^0 specimen is expected to follow a linear function (Equation (1)).

$$[Fe] = k_{EDTA} * t + b \quad (1)$$

The regression parameters of the experimental data (k_{EDTA} and "b") are characteristic for each Fe^0 [47,63]. Direct comparison of the calculated rates of iron dissolution (k_{EDTA}) could be used to indicate the more reactive SW materials, while the calculated intercept ('b') values could be used to indicate the relative amount of pre-existing corrosion products present on the material surfaces. Linear parameters were determined using the Origin graphing software.

2.5.2. Removal Efficiency (E Value)

The changes in magnitude of the tested systems for MB discoloration and water defluoridation were calculated and presented as efficiency percentages (E value). Initial (C_0) and final (C) concentration of the species were determined, and the following formula was used to calculate the removal efficiency:

$$E = [1 - (C/C_0)] * 100\% \quad (2)$$

The operational initial concentration (C_0) for each case was acquired from a triplicate control experiment without additive material (blank). This procedure was mainly to account for experimental errors due to dye adsorption onto the walls of the test tubes.

3. Results and Discussion

3.1. Iron Dissolution in EDTA

3.1.1. Appropriateness of the Experimental Approach

Figure 2 compares the results of iron dissolution in 2 mM EDTA for three Fe^0 SW and the GI. EDTA clearly dissolves far more iron from Fe^0 SW than from GI. The Fe dissolution kinetics was more rapid for SW as well. The deferential behaviour from Figure 2 is explained by considering the chemistry of the system. In fact, Fe^0 is corroded by water (H_2O or H^+) according to Equation (3). Generated Fe^{2+} is further oxidized to Fe^{3+} ions by dissolved O_2 (Equation (4)). In essence, Fe^{3+} is available as $Fe(H_2O)_6{}^{3+}$ which tend to polymerize and precipitate as $Fe(OH)_3$ but under the conditions of this study H_2O is replaced by EDTA that form very stable complexes with Fe^{3+} (Equation (5)) [64,65]. In other words, $Fe(OH)_3$ precipitation will not occur before the solution is saturated ([Fe] = 112 mg L^{-1}). Figure 2 shows that for the SW specimens, saturation occurs after 50 h and [Fe] = f(t) is no more linear. For GI no saturation occurs even after 140 h.

$$Fe^0 + 2\,H^+ \Rightarrow Fe^{2+} + H_2 \quad (3)$$

$$4\,Fe^{2+} + 2\,H^+ + O_2 \Rightarrow 4\,Fe^{3+} + 2\,OH^- \quad (4)$$

$$Fe^{3+} + EDTA \Rightarrow Fe(EDTA)^{3+} \quad (5)$$

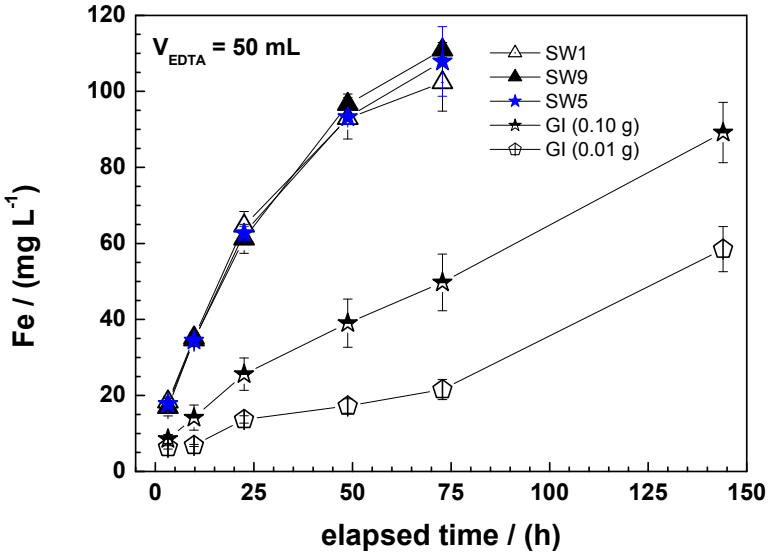

Figure 2. Time-dependent iron dissolution from (i) 0.01 g of SW1, SW5, and SW9 and (ii) 0.01 and 0.10 g of granular iron (GI). All regression parameters for 0.01 g Fe^0 are listed in Table 3. The represented lines are not fitting functions, they just join the points to facilitate visualization.

Table 3. Corresponding correlation parameters (k_{EDTA}, b, R^2) for SW1–SW12 and granular iron. As a rule, the more reactive a material is under given conditions, the higher the k_{EDTA} value. R^2 is a correlation factor. General conditions: 50 mL of 2 mM EDTA solution and 0.01 g Fe^0. K_{EDTA}, b, and R^2 were calculated using Origin 8.0.

Fe^0	k_{EDTA}	b	R^2
	(μg h^{-1})	(μg)	(–)
SW 1	78.4	552.9	0.8851
SW 2	111.7	160.0	0.9984
SW 3	113.0	435.8	0.9761
SW 4	110.9	322.4	0.9873
SW 5	106.9	393.0	0.9707
SW 6	130.8	282.6	0.9881
SW 7	112.6	261.6	0.9960
SW 8	0.0	0.0	n.a.
SW9	84.9	289.4	0.9944
SW10	108.3	516.7	0.9970
SW11	0.0	0.0	n.a.
SW12	28.7	77.9	0.9838
SW13	31.2	−170.8	0.8010
SW14	24.4	−138.4	0.9583
SW15	20.1	132.6	0.7427
GI	3.7	−10.3	0.9396

Fe^0 oxidative dissolution in water or aqueous iron corrosion is spontaneous because the electrode potential of water (E^0 = 0.00 V for H^+/H_2) is larger than that of Fe^0 (E^0 = −0.44 V). However, E^0 = −0.44 V is valid for all reactive Fe^0-bearing materials. In other words, material specific characteristics will determine the kinetics of Fe^0 dissolution. Dannenberg and Potter [15] reported on specific surface areas

(SSA) of 120, 100, and 50 cm^2 for grades 0 (d = 50 μm), 1 (d = 60 μm), and 2 (d = 75 μm) Fe^0 SW. This suggests that, rooting the reasoning on the SSA alone, a reactivity ratio of 2 is expected when grades 1 and 2 are used in any application. There are seven classes of Fe^0 SW depicting thicknesses of the SW filament (d) varying from 25 to 100 μm [12]. Therefore, it is essential to comparatively characterize their reactivity in order to ease their selection for site-specific designs.

Figure 2 clearly shows that GI is dissolved with a far lower dissolution rate than the three presented SW specimens. Two different masses of GI are used (0.1 and 0.01 g) while the used mass of SW was 0.01 g. With regard to the linearity of the [Fe] = f(t) function, it is evident that longer experimental durations are needed for GI (up to four days) while SW characterization is achieved within 24 h. Previous works have demonstrated that the linearity of Equation (1) is difficult to be obtained with fine Fe^0 materials and with those covered with iron corrosion products. The reason being that EDTA dissolves Fe^{III} species as well [12]. The next section presents the tools utilized herein to obtain reasonable k_{EDTA} values. It should be explicitly stated that Figure 2 illustrates the differential behaviour of SW and GI. The expected trend of more rapid Fe dissolution from smaller particles is documented. The next result is that material of diverse coarseness cannot be characterized under the same experimental conditions using the EDTA test [12].

3.1.2. k_{EDTA} Values

The results of the conventional EDTA test (0.1 g Fe^0, four days) for SW1 to SW8 are summarized in Figure 3a. Except from nonreactive SW8 (stainless steel), all materials depicted very similar dissolution rates and therefore are not easily distinguishable. There is no linear trend in the dissolution rates of all reactive SW specimens, which makes classification of dissolution efficiency impossible. The cause for the nonlinearity is the higher reactivity of SW and the presence of atmosphereic FeCPs on their surface [12,47]. Two major modifications were made to achieve reasonable k_{EDTA} values: (i) Lowering the mass of Fe^0 SW to 0.04 and 0.01, and increasing the volume of the EDTA solution to 100 mL [45]. The tested materials could be roughly grouped in three different classes: (i) Nonreactive (SW8), (ii) low reactive (SW1, SW2, SW3, SW4), and (iii) very reactive (SW5, SW6, SW7). After achieving optimal test conditions with the 8 Fe^0 SW the remaining seven specimens and GI were tested using 0.01 g SW and 50 mL of the EDTA solution (Figure 3b). The results for all tested 16 Fe^0 specimens are summarized in Table 3.

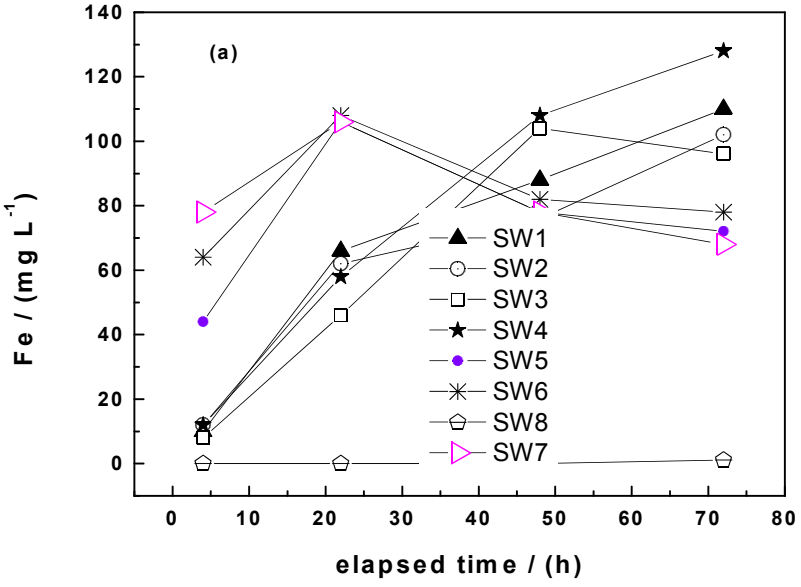

Figure 3. *Cont.*

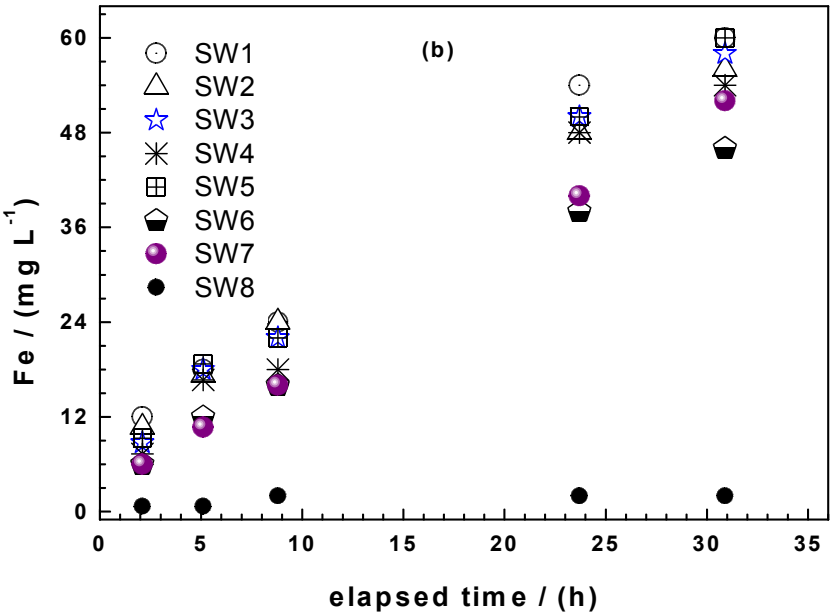

Figure 3. Comparison of the dissolution rate of eight steel wool specimens (SW1 to SW8) in 50 mL of a 2 mM ethylenediaminetetraacetate (EDTA) solution under quiescent conditions for up to 70 h. Experimental conditions: (**a**) m_{SW} = 0.10 g, and (**b**) m_{SW} = 0.01 g. The represented lines are not fitting functions; they just connect the points to ease visualization.

Figure 3b shows clearly that: (i) SW8 is nonreactive, (ii) SW6 and SW7 are less reactive than the five other materials, and (iii) the reactivity of the five remaining materials cannot be visually achieved. The regression parameters for all tested materials are summarized in Table 3 and the value of k_{EDTA} is used to classify the reactivity of the Fe^0 SW which are collectively far higher than that of GI. Table 3 shows that SW8 and SW 11 are nonreactive. The k_{EDTA} values for SW12 to SW15 were lower than 30 μg h^{-1} and they are considered as low reactive. The k_{EDTA} values for SW1 and SW9 are 78.4 and 84.9 μg h^{-1}, respectively, they are operationally considered as middle reactive. For the remaining Fe^0 SW specimens the k_{EDTA} values were larger than 100 μg h^{-1} and they are considered as very reactive. The remaining reasoning is focused on SW1 to SW7 while considering SW8 and GI as "negative" reference. Low reactive Fe^0 SW were also not further considered because they were all not from the local marked (Table 1). The objective of leaching in column studies was to check whether a better differentiation of three materials (SW5, SW6, and SW7) from the class "very reactive" was possible. For comparison one "middle reactive" material (SW1) and GI were considered.

3.1.3. Column Leaching Studies

Figure 4a shows that the four Fe^0 SW exhibited markedly increased iron dissolution during the whole experiments (53 leaching events) than GI. It is also seen that there are picks in the iron concentration. Hildebrant [45] demonstrated that the picks did not correspond to longer standing times (e.g., weekends values with 72 h of equilibration). It is also seen that the saturation value (112 mg L^{-1}) for iron was never achieved. The last important observation from Figure 4a is that there are waves in the kinetics of iron dissolution. The most remarkable pick is the one for GI around the 20th leaching event. Here, GI suddenly release more Fe than SW6 which is the most reactive material according to the k_{EDTA} values. It is not worth trying to rationalize this behaviour, it is enough to document it at this stage and look in the future if such results are reported. Similarly as the EDTA test, absolute Fe concentrations are needed to differentiate the reactivity of the Fe^0 SW.

Figure 4b summarizes the cumulative amount of Fe leached from each column. GI is the least reactive material for the whole 53 leaching events. Interestingly, until the 6th event, all the four Fe^0 SW specimens behaved very similarly with SW7 releasing slightly more iron. Afterwards, SW7 was constantly the most reactive material while SW1 and SW5 behaved very similarly and constantly better than SW6. In other words, SW6, the best material according to the k_{EDTA} value, is the least reactive from the 4 Fe^0 SW considered in column leaching experiments. This observation corroborates the need for long-term experiments in testing Fe^0 materials for environmental remediation and water treatment.

Another important issue from Figure 4b is the change of the slopes of all materials: For GI already after some five leaching events, for SW1 after 16 leaching events and for the three other after 40 events. These results elegantly demonstrate the nonlinearity of the kinetic of iron corrosion under conditions where there is no oxide scale on Fe^0. Under field conditions, the precipitation of iron hydroxide and the myriad of processes that influence its stability are certainly as site-specific as the water to be treated. For this reason at least, there should be unified reductionists protocol to characterize the intrinsic reactivity of Fe^0 materials relevant for field applications.

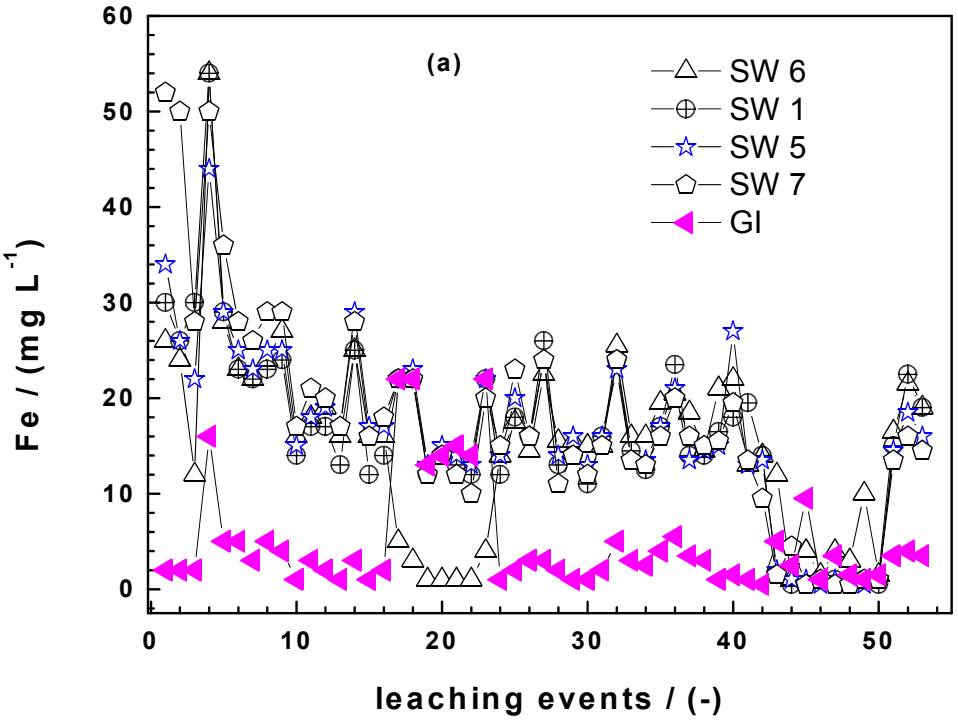

Figure 4. *Cont.*

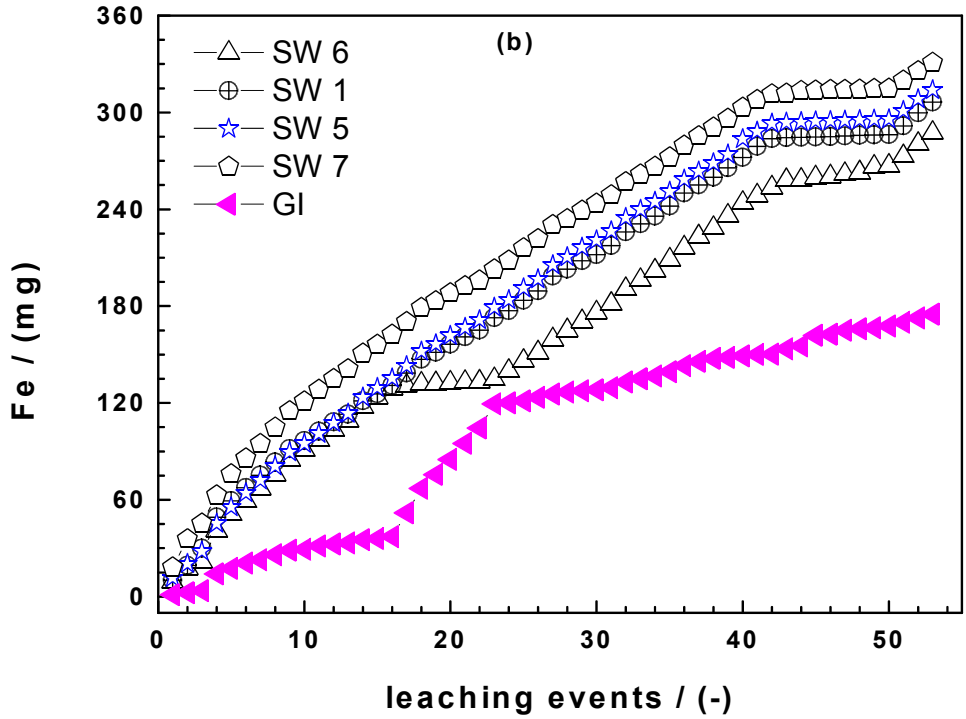

Figure 4. Comparison of the extent of iron dissolution in column leaching experiments for SW1, SW5, SW6, SW7, and GI: (**a**) Iron concentration and (**b**) cumulative mass of dissolved iron. Experimental conditions: m_{iron} = 0.500 g, [EDTA] = 2 mM.

3.2. MB Discoloration

Figure 5a summarizes the results of MB discoloration after two weeks. It confirms that SW8 is not reactive and Fe^0 SW perform better than GI. From the Fe^0 SW specimens, SW5 performed the best. SW1, SW3, and SW4 were very similar in their E values and performed slightly lower than SW6, SW2, and SW7. It is recalled that only grade 00 (fine—d = 40 μm) materials were used in column leaching experiments (Table 1), together with GI. The order of efficiency as related by the mean E values is the following:

GI < SW1 (d = 40 μm) < SW3 < SW4 < SW6 (d = 40 μm) < SW2 < SW7 (d = 40 μm) < SW5 (d = 40 μm), following the extent of Fe leaching in columns the order was:

GI < SW6 (d = 40 μm) < SW1 (d = 40 μm) < SW5 (d = 40 μm) < SW7 (d = 40 μm).

The only constant for both classifications is that GI is the least performant material. However, considering the standard deviations (error bars), the classification of MB discoloration can be rewritten as:

GI < SW1 ≅ SW3 ≅ SW4 ≅ SW6 < SW2 ≅ SW7 ≅ SW5.

Accordingly, there is a direct correlation between the extent of iron dissolution and the extent of MB discoloration. This correlation is obvious, given that MB is mainly removed by coprecipitation with FeCPs of very low affinity to MB. Under the same experimental conditions, Hildebrant [45] reported on quantitative removal of methyl orange with no significant difference is the E values for all Fe^0 SW specimens.

Figure 5b summarizes the results of MB discoloration after eight weeks (two months). It is seen that the longer experimental duration enabled quantitative MB discoloration by all Fe^0 SW specimens. The main feature from Figure 5b is that whenever enough FeCPs is produced, contaminant removal is quantitative. Actually, Fe^0 materials are used for water treatment without any idea on their intrinsic reactivity nor their long-term kinetics of corrosion. This is the main reason why despite 170 years of technical expertise, designing an efficient and sustainable system is still an exception.

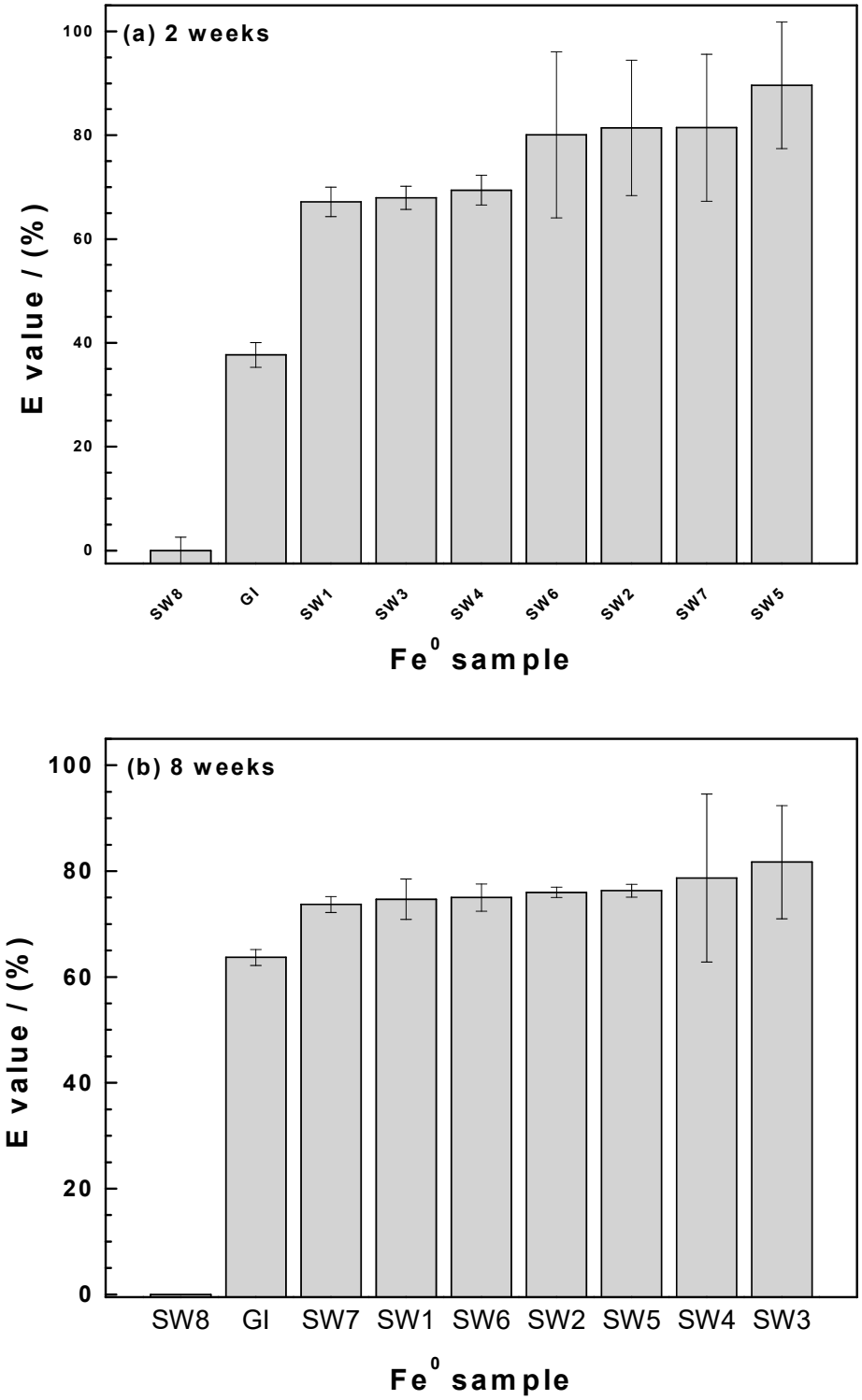

Figure 5. Extent of methylene blue discoloration for SW1–SW8 and GI after (**a**) two weeks and (**b**) eight weeks. Experimental conditions: 0.05 g Fe^0; V = 22 mL; [MB] = 10 mg/L; rotational shaking at 75 rotations per min.

3.3. Water Defluoridation

3.3.1. Batch Experiments

Figure 6a summarizes the results of fluoride removal in quiescent batch experiments for two weeks. The results depict very limited water defluoridation (E < 20%). This corroborates recent results by [66–68]. Knowing the less efficiency of GI for F^- removal, the experiments were designed to investigate whether filamentous SW can perform better. The order of reactivity based on the mean values in Figure 6a enables the following order of reactivity:

SW8 (nonreactive) < SW7 < SW6 < SW3 < SW4 < SW5 < SW2 < SW1

It is surprising that SW1, representative for the "low reactive" materials exhibited the highest removal performance. The difference is significant even when the standard deviation is considered. This is another reproducible result, that can only be documented while hoping that future works would enable a better explanation. The impression here is that it seems that the most reactive material is not the best for water defluoridation. This would suggest that coprecipitation is not the main removal mechanism or that nascent iron hydroxides cannot not mediate F^- removal. The results of column experiments seem to confirm this trend.

3.3.2. Column Experiments

Figure 6b summarizes the results of fluoride removal in column experiments for 44 leaching events. It is seen that the best fluoride removal for each system was achieved during the very first leaching even, reaching 70% for SW1. Afterwards, E decreased to values lower than 30% with two picks at (E > 30%) at the 27th and the 40th leaching event. In these two situations, SW1 was constantly the best material. Hildebrant [45] calculated the cumulative percent F^- removal during the whole leaching experiments and obtained the following results:

SW1 (18.3%) < SW2 (16.6%) < SW3 (15.2%) < SW4 (12.3%) < SW6 (11.2%).

These results suggest that fluoride removal by ion exchange onto "aged" FeCPs is more important than fluoride coprecipitation with nascent iron hydroxides. This observation excellently explained the results of Heimann [66] who documented 20% fluoride removal in a column experiment using 100 g of the GI used herein and no removal while changing the water flow velocity. More importantly, these results explain the enigma, why aged iron oxides and laterite are efficient for water defluoridation and Fe^0 not (or less) as summarized in Heimann et al. [67].

Figure 6b also confirms "waves" in the kinetics of Fe^0 SW efficiency with the net difference that maxima correspond to minima in the EDTA leaching experiments. The most important information from these investigations is that it is possible to manufacture specific iron oxides for water defluoridation [69]. Whenever this would not be affordable for small communities, it would be an attractive process for industrial and mining wastewater.

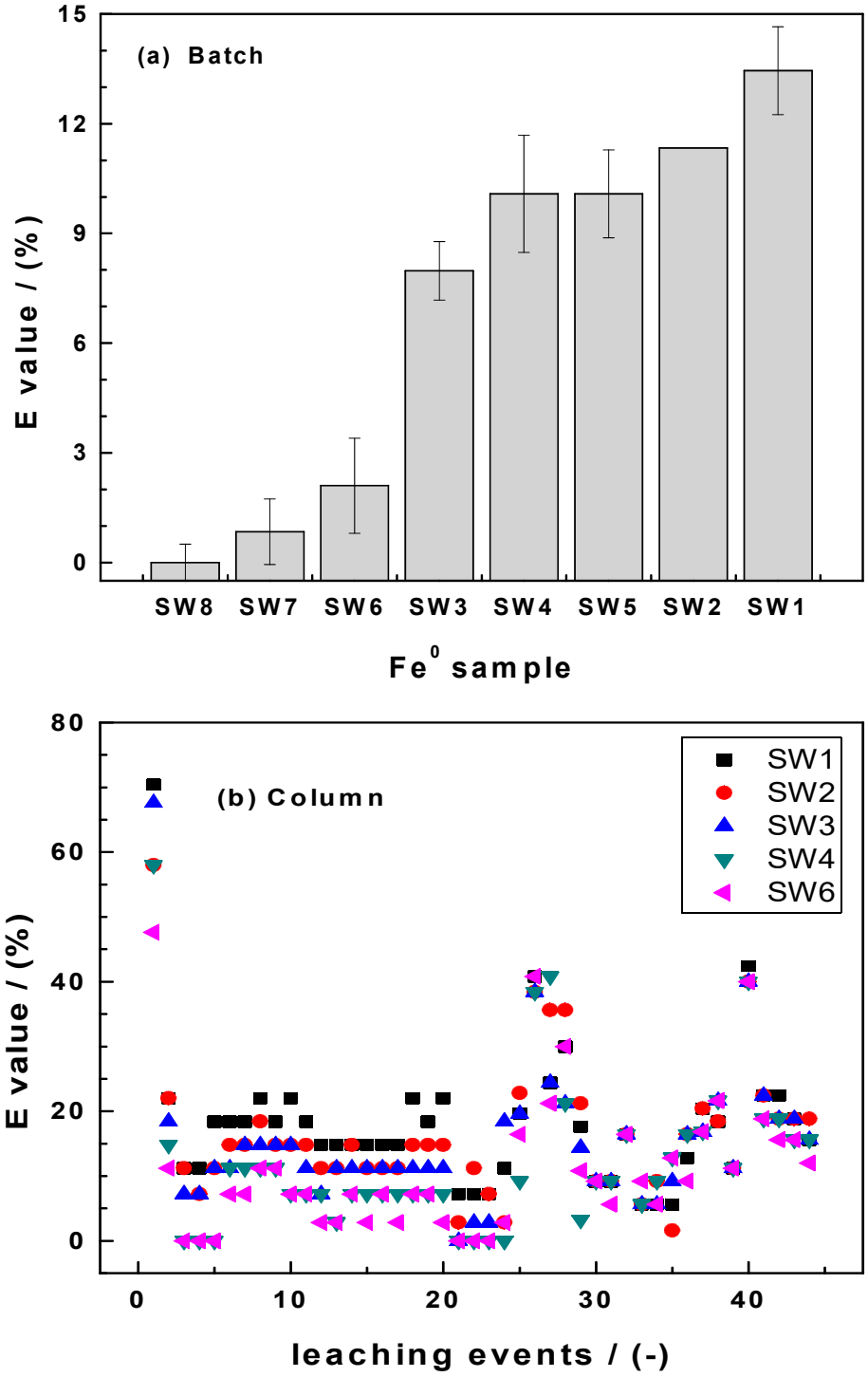

Figure 6. Extent of water defluoridation in (**a**) batch experiments and (**b**) intermittent column filtration. Experimental column conditions: 2.0 g Fe^0 SW; V = 22 mL; $[F^-]$ = 25 mg/L.

3.4. Discussion

3.4.1. Research in Progress

The efficiency of Fe^0/H_2O systems for water treatment under natural conditions (pH > 5.0) is influenced by a myriad of factors, of which the presence and the amount of dissolved O_2 can be regarded as the most important [70]. A Fe^0/H_2O system is grounded on a redox process which is Fe^0

oxidative dissolution by water (H^+ or H_2O). Fe^0 is oxidized by water and its surface is covered by an oxide scale containing reducing agents (e.g., H_2, Fe^{II}, and Fe^{II}/Fe^{III} species). The nature and the permeability of the oxide scale depend on the abundance of dissolved O_2 [71,72]. The abundance and the nature of iron hydroxides and oxides within the oxide scale influence the efficiency of each system for water treatment and additionally depends on the nature of the contaminants (e.g., speciation) [59].

The low adsorptive affinity of methylene blue (MB) for the oxide scale (on Fe^0) has been almost routinely used to characterize the dynamic nature of the Fe^0/H_2O system [47,49]. The present study has identified water defluoridation as another reactive tracer for the Fe^0/H_2O system. Fluoride removal by nascent iron hydroxide is absolutely nonfavorable while MB discoloration occurs at a low rate. Thus, combining the two tools in long term column experiments seems to be the new avenue to investigate the long-term efficiency of Fe^0/H_2O systems in an affordable manner. The affordability of the approach results from the fact that just a fluoride electrode is added to the standard laboratory equipment. MB discoloration and water defluoridation identify waves in the iron dissolution kinetics, re-demonstrating the nonlinear nature of the kinetic of iron corrosion [73]. Moreover, the results suggest that iron corrosion in a field Fe^0/H_2O system is a stochastic process [49] which should be better characterize before been implemented in predictive models. This is probably the next major challenge of the Fe^0 remediation research community as Santisukkasaem and Das [74] recently demonstrated the inadequacy of all available models to cope with the complex nature of the Fe^0/H_2O system. However, the nondimensional analysis of the permeability loss they suggested is equally not a stand-alone solution because the real cause of permeability loss is not important for their model. Before moving to such simplistic models, a science-based analysis of the Fe^0/H_2O system should be performed. In these investigations the nonlinear kinetic of Fe^0 corrosion should be given a capital importance.

Properly selecting the material used in individual applications is very important. For example, while testing Fe^0 SW for household water treatment, Bradley et al. [42] realized that there was a Fe^0 complete depletion of grade 0000 (extra fine—d = 25 μm) after six months (170 days). Tepong-Tsindé et al. [43] tested grade 0 (fine—d = 50 μm) for 12 months and have not achieved any material depletion. The four Fe^0 SW (Table 1) tested in column leaching experiments herein were depleted to 57.5% to 66.2% after 53 leaching even. Future work should identify the time frame (or the number of leaching events) needed for complete depletion of various classes of Fe^0 SW using the EDTA and the Phen leaching experiments [12]. The results of such experiments would be a better way to predict the service life of Fe^0 SW specimens than each theoretical estimation. Moreover, characterized materials will be also useful for other applications (e.g., biogas purification) [75–77].

Fe^0 SW has been suggested and used for H_2S removal from biogas [75–77]. The work conducted until now to identify the characteristics of these materials for the named application has not been systematic. In particular, SW selection was not addressed. For example, photographs presented by Magomnang and Villanueva [76] suggest that the material they used was close to SW12 tested herein (Table 1) and characterized as "low reactive". This suggests that, following the principle of Notter [4] it suffices to work with the same design while using a more reactive material (e.g., SW7) to achieve a better quality of biogas. Clearly the tool presented herein will also facilitate the design of Fe^0-based filters for biogas purification. Another important field of application is the production of small amounts of H_2 to initiate biological processes (e.g., at laboratory scale) [refs].

3.4.2. Significance of the Results

Metallic iron is oxidized in Fe^0/H_2O systems to ferrous ion and H_2. Ferrous ion migrates and precipitates at the surface of other aggregates (e.g., in situ coating of sand or zeolite). Iron oxide coated aggregates fix contaminants by adsorption and coprecipitation. In column systems, iron oxides fill the porous volume and improve contaminant removal by size-exclusion [78–80]. That is the thermodynamic of all Fe^0/H_2O systems. It should be added that Fe^0 corrosion in an O_2 scavenging process implying that oxidation of Fe^0 contributes to produce anoxic conditions [81]. The extent to which O_2 scavenging is achieved implies that some removal processes (e.g., denitrification) are just

indirectly mediated [43]. In other words, the thermodynamic of the Fe^0/H_2O system implies that Fe^0 can be universally used for: (i) H_2 generation, (ii) O_2 consumption, and (iii) generation of FeCPs (iron hydroxides and oxides). FeCPs are contaminant scavengers and this property was documented for a very long time [1]. The fact that some contaminants are reduced in Fe^0/H_2O systems is not discussed herein. It is just recalled that H_2 and Fe^{II} and Fe^{II}/Fe^{III} species are stand-alone reducing agents [28,79,80]. The open question is how to design an efficient and sustainable Fe^0/H_2O system.

The efficiency of a Fe^0/H_2O system for water decontamination primary depends on three key factors: (i) The nature and the extent of water contamination, (ii) the extent to which decontamination should occur, and (iii) the rate at which contaminant scavengers (here FeCPs) are made available. Previous works have paid clearly low attention to the corrosion rates. This study shows that, the k_{EDTA} values for the tested Fe^0 SW varies from 20.1 to 130.8 μg h^{-1} (Table 3). This corresponds to a reactivity ratio of about 1/6. However, the k_{EDTA} values were determined in experiments lasting for just three days and correspond at best to the initial kinetics of iron corrosion which is well-known to be nonlinear [43,73]. The results of long-term leaching presented herein (Section 3.1.3) have documented waves (even) in this initial corrosion rate. Therefore, it is imperative to characterize the long-term reactivity of Fe^0 materials, including Fe^0 SW.

There have been very scare attempts to systematically characterize the effects of operational parameters on the efficiency of Fe^0/H_2O systems for water treatment. To the best of the author's knowledge, Dannenberg and Potter [15] have presented the most extensive investigations for Fe^0 SW. The authors devised and successfully tested a Fe^0 SW based system for the recovery of silver from waste solutions. The following operational parameters were characterized at laboratory and pilot scale testing: (i) The SW grade or type (e.g., coarseness of filaments), (ii) the pH of the wastewater, (iii) the solution chemistry (e.g., concentrations of major ions), (iv) the flow rate, (v) the flow continuity (continuous flow versus intermittent), (vi) the packing density in the Fe^0 SW units, and (vi) the size of the Fe^0 SW units. In particular, Dannenberg and Potter [15] tested SW grades 0, 1, and 2 having approximate specific surface areas of 120, 100, and 50 cm^2 g^{-1} respectively and established that the Fe^0 SW size do affect the decontamination capacity. The most important information from Dannenberg and Potter [15] is that, under specific conditions, the SW grade is a stand-alone efficiency parameter. The results of MB and MO discoloration achieved by Hildebrant [45] demonstrate how the nature of the contamination is essential in designing an efficient system. Even the results of water defluoridation presented herein confirm this assertion. In essence, given that it is the aqueous iron corrosion that implies decontamination, the sole open issue is designing efficient systems and this was already postulated in 1878 by Notter [4].

According to Notter [4], the success of any designed filter depends on: (i) The quantity and quality of the water to be treated, (ii) the characteristics of the filtering media, (iii) the speciation of the contaminants(s), and (iv) the regenerability of the filtering material readily. Applying the principles to Fe^0-based filters, it could be said that it is time to apply this 140-year-old principle. In particular, which amount of Fe^0 material? Which mixing ratio? Which bed length or how many columns? For which volume of clean water per unit time (day, hour)? Required experiments should last for long times (at least one year) as there is no way to reproduce accelerated iron corrosion. The authors have been advocating for the past decade that designing such filters will universally provide safe drinking water to low-income communities worldwide [82–84].

4. Conclusions

The modified EDTA test provides an accurate and reliable tool to assess the intrinsic reactivity of Fe^0 SW. The experiment is accomplished within two days and needs only a UV/vis spectrophotometer. Results from the EDTA test are corroborated by the MB test and by water defluoridation. The combination of the three methods provides a facile way to demonstrate the nonlinear nature of the corrosion rate. In particular, the results unambiguously established that water defluoridation with conventional Fe^0 materials would be a laborious task. The combination of the three methods

appears to be a reliable way to discuss the suitability of Fe^0 materials for various applications. Future works should reproduce these experiments for longer experimental duration to use their full capacity in facilitating suitable materials for site-specific applications. The named combination of the three methods is also regarded as a universal testing procedure to evaluate new Fe^0 for environmental applications (quality control).

Author Contributions: B.H., A.I.N.-T., M.L., T.L., and C.N. contributed equally to manuscript compilation and revisions. All authors have read and agreed to the published version of the manuscript.

Funding: This research has received no funding.

Acknowledgments: The manuscript was improved by insightful comments of anonymous reviewers from Processes. We acknowledge support by the German Research Foundation and the Open Access Publication Funds of the Göttingen University.

Conflicts of Interest: The authors declare no conflict of interest.

References

1. Bischof, G. *The Purification of Water: Embracing the Action of Spongy Iron on Impure Water*; Bell and Bain: Glasgow, UK, 1873; 19p.
2. Bischof, G. On putrescent organic matter in potable water. *Proc. R. Soc. Lond.* **1877**, *26*, 258–261.
3. Bischof, G. On putrescent organic matter in potable water II. *Proc. R. Soc. Lond.* **1878**, *27*, 152–156.
4. Notter, J.L. The purification of water by filtration. *Br. Med. J.* **1878**, *12*, 556–557. [CrossRef]
5. Nichols, W.R. *Water Supply, Considered Mainly from a Chemical and Sanitary Standpoint*; John Wiley & Sons: New York, NY, USA, 1883; 260p.
6. Anderson, W. On the purification of water by agitation with iron and by sand filtration. *J. Soc. Arts* **1886**, *35*, 29–38. [CrossRef]
7. Devonshire, E. The purification of water by means of metallic iron. *J. Frankl. Inst.* **1890**, *129*, 449–461. [CrossRef]
8. Antia, D.D.J. Sustainable zero-valent metal (ZVM) water treatment associated with diffusion, infiltration, abstraction and recirculation. *Sustainability* **2010**, *2*, 2988–3073. [CrossRef]
9. Baker, M. Sketch of the history of water treatment. *Am. Water Works Assoc.* **1934**, *26*, 902–938. [CrossRef]
10. Van Craenenbroeck, W. Easton & Anderson and the water supply of Antwerp (Belgium). *Ind. Archaeol. Rev.* **1998**, *20*, 105–116.
11. Mwakabona, H.T.; Ndé-Tchoupé, A.I.; Njau, K.N.; Noubactep, C.; Wydra, K.D. Metallic iron for safe drinking water provision: Considering a lost knowledge. *Water Res.* **2017**, *117*, 127–142. [CrossRef]
12. Lufingo, M.; Ndé-Tchoupé, A.I.; Hu, R.; Njau, K.N.; Noubactep, C. A novel and facile method to characterize the suitability of metallic iron for water treatment. *Water* **2019**, *11*, 2465. [CrossRef]
13. Ndé-Tchoupé, A.I. Design and Construction of Fe^0-Based Filters for Hhouseholds. Ph.D. Thesis, University of Douala, Douala, Cameroon, 2019. (In French).
14. Lufingo, M. Investigation of Metallic Iron for Water Defluoridation. Master's Thesis, Nelson Mandela African Institution of Science and Technology, Arusha, Tanzania, 2020.
15. Dannenberg, R.O.; Potter, G.M. *Silver Recovery from Waste Photographic Solutions by Metallic Displacement*; Report of Investigations 7117; BuMines: Washington, DC, USA, 1968; 22p.
16. Anderson, M.A. *Fundamental Aspects of Selenium Removal by Harza Process*; Rep San Joaquin Valley Drainage Program; US Dep Interior: Sacramento, CA, USA, 1989.
17. Martins, G.F. Percent oxygen in air. *J. Chem. Educ.* **1987**, *64*, 809. [CrossRef]
18. Gordon, J.; Chancey, K. Steel wool and oxygen: A look at kinetics. *J. Chem. Educ.* **2005**, *82*, 1065. [CrossRef]
19. Vogelezang, M. Steel wool and oxygen: How constant should a rate constant be? *J. Chem. Educ.* **2006**, *83*, 214. [CrossRef]
20. Vera, F.; Rivera, R.; Núñez, C. A simple experiment to measure the content of oxygen in the air using heated steel wool. *J. Chem. Educ.* **2011**, *88*, 1341–1342. [CrossRef]
21. Lauderdale, R.A.; Emmons, A.H. A method for decontaminating small volumes of radioactive water. *J. Am. Water Works Assoc.* **1951**, *43*, 327–331. [CrossRef]

22. Lacy, W.J. Removal of radioactive material from water byslurrying with powdered metal. *J. Am. Water Works Assoc.* **1952**, *44*, 824–828. [CrossRef]
23. Sifrin, S.M.; Spivakova, O.M.; Krasnoborod'ko, I.G. On color removal from textile wastewater. *Sel. Pap. Leningr. Civ. Eng. Inst.* **1971**, *69*, 112–119.
24. Sugimoto, S.; Sakaki, T. Study on decontamination of radioactive ruthenium by steel wool in waste solution. *Radioisotopes* **1979**, *28*, 361–366. [CrossRef]
25. Tseng, C.L.; Yang, M.H.; Lin, C.C. Rapid determination of cobalt-60 in sea water with steel wool adsorption. *J. Radioanal. Nucl. Chem. Lett.* **1984**, *85*, 253–260. [CrossRef]
26. Albinsson, Y.; Christiansen-Saetmark, B.; Engkvist, I.; Johansson, W. Transport of actinides and Technetium through a bentonite backfill containing small quantities of iron or copper. *Radiochim. Acta* **1991**, *52–53*, 283.
27. Khudenko, B.M. Feasibility evaluation of a novel method for destruction of organics. *Water Sci. Technol.* **1991**, *23*, 1873–1881. [CrossRef]
28. Gould, J.P. The kinetics of hexavalent chromium reduction by metallic iron. *Water Res.* **1982**, *16*, 871–877. [CrossRef]
29. Erickson, A.J. Enhanced Sand Filtration for Storm Water Phosphorus Removal. Master's Thesis, University of Minnesota, Minneapolis, MN, USA, 2005.
30. Erickson, A.J.; Gulliver, J.S.; Weiss, P.T. Enhanced sand filtration for storm water phosphorus removal. *J. Environ. Eng.* **2007**, *133*, 485–497. [CrossRef]
31. Erickson, A.J.; Gulliver, J.S.; Weiss, P.T. Phosphate removal from agricultural tile drainage with iron enhanced sand. *Water* **2017**, *9*, 672. [CrossRef]
32. Del Cul, G.D.; Bostick, W.D.; Trotter, D.R.; Osborne, P.E. Technetium-99 removal from process solutions and contaminated groundwater. *Sep. Sci. Technol.* **1993**, *28*, 551–564. [CrossRef]
33. Del Cul, G.D.; Bostick, W.D. Simple method for technetium removal from aqueous solutions. *Nucl. Tecknol.* **1995**, *101*, 161. [CrossRef]
34. James, B.R.; Rabenhorst, M.C.; Frigon, G.A. Phosphorus sorption by peat and sand amended with iron oxides or steel wool. *Water Environ. Res.* **1992**, *64*, 699–705. [CrossRef]
35. Ndé-Tchoupé, A.I.; Crane, R.A.; Mwakabona, H.T.; Noubactep, C.; Njau, K.N. Technologies for decentralized fluoride removal: Testing metallic iron based filters. *Water* **2015**, *7*, 6750–6774. [CrossRef]
36. Campos, V. The effect of carbon steel-wool in removal of arsenic from drinking water. *Environ. Geol.* **2002**, *42*, 81–82. [CrossRef]
37. Cornejo, L.; Lienqueo, H.; Arenas, M.; Acarapi, J.; Contreras, D.; Yáñez, J.; Mansilla, H.D. In field arsenic removal from natural water by zero-valent iron assisted by solar radiation. *Environ. Pollut.* **2008**, *156*, 827–831. [CrossRef]
38. Özer, A.; Altundogan, H.S.; Erdem, M.; Tümen, F. A study on the Cr(VI) removal from aqueous solutions by steel wool. *Environ. Pollut.* **1997**, *97*, 107–112. [CrossRef]
39. Gromboni, C.F.; Donati, G.L.; Matos, W.O.; Neves, E.F.A.; Nogueira, A.R.A.; Nobrega, J.A. Evaluation of metabisulfite and a commercial steel wool for removing chromium (VI) from wastewater. *Environ. Chem. Lett.* **2010**, *8*, 73–77. [CrossRef]
40. Till, B.A.; Weathers, L.J.; Alvarez, P.J.J. Fe(0)-supported autotrophic denitrification. *Environ. Sci. Technol.* **1998**, *32*, 634–639. [CrossRef]
41. Lavania, A.; Bose, P. Effect of metallic iron concentration on end-product distribution during metallic iron-assisted autotrophic denitrification. *J. Environ. Eng.* **2006**, *132*, 994–1000. [CrossRef]
42. Bradley, I.; Straub, A.; Maraccini, P.; Markazi, S.; Nguyen, T.H. Iron oxide amended biosand filters for virus removal. *Water Res.* **2011**, *45*, 4501–4510. [CrossRef] [PubMed]
43. Tepong-Tsindé, R.; Ndé-Tchoupé, A.I.; Noubactep, C.; Nassi, A.; Ruppert, H. Characterizing a newly designed steel-wool-based household filter for safe drinking water provision: Hydraulic conductivity and efficiency for pathogen removal. *Processes* **2019**, *7*, 966. [CrossRef]
44. Li, Z.; Huang, D.; McDonald, L.M. Heterogeneous selenite reduction by zero valent iron steel wool. *Water Sci. Technol.* **2017**, *75*, 908–915. [CrossRef]
45. Hildebrant, B. Characterizing the reactivity of commercial steel wool for water treatment. *Freib. Online Geosci.* **2018**, *53*, 1–60.
46. Mitchell, G.; Poole, P.; Segrove, H.D. Adsorption of methylene blue by high-silica sands. *Nature* **1955**, *176*, 1025–1026. [CrossRef]

47. Btatkeu-K, B.D.; Miyajima, K.; Noubactep, C.; Caré, S. Testing the suitability of metallic iron for environmental remediation: Discoloration of methylene blue in column studies. *Chem. Eng. J.* **2013**, *215–216*, 959–968.
48. Miyajima, K.; Noubactep, C. Impact of Fe^0 amendment on methylene blue discoloration by sand columns. *Chem. Eng. J.* **2013**, *217*, 310–319. [CrossRef]
49. Miyajima, K. Optimizing the design of metallic iron filters for water treatment. *Freib. Online Geosci.* **2012**, *32*, 1–60.
50. Reardon, J.E. Anaerobic corrosion of granular iron: Measurement and interpretation of hydrogen evolution rates. *Environ. Sci. Technol.* **1995**, *29*, 2936–2945. [CrossRef] [PubMed]
51. Reardon, E.J. Zerovalent irons: Styles of corrosion and inorganic control on hydrogen pressure buildup. *Environ. Sci. Tchnol.* **2005**, *39*, 7311–7317. [CrossRef] [PubMed]
52. Miehr, R.; Tratnyek, G.P.; Bandstra, Z.J.; Scherer, M.M.; Alowitz, J.M.; Bylaska, J.E. Diversity of contaminant reduction reactions by zerovalent iron: Role of the reductate. *Environ. Sci. Technol.* **2004**, *38*, 139–147. [CrossRef] [PubMed]
53. Kim, H.; Yang, H.; Kim, J. Standardization of the reducing power of zero-valent iron using iodine. *J. Environ. Sci. Health A* **2014**, *49*, 514–523. [CrossRef]
54. Li, S.; Ding, Y.; Wang, W.; Lei, H. A facile method for determining the Fe(0) content and reactivity of zero valent iron. *Anal. Methods* **2016**, *8*, 1239–1248. [CrossRef]
55. Li, J.; Dou, X.; Qin, H.; Sun, Y.; Yin, D.; Guan, X. Characterization methods of zerovalent iron for water treatment and remediation. *Water Res.* **2019**, *148*, 70–85. [CrossRef]
56. Miyajima, K.; Noubactep, C. Effects of mixing granular iron with sand on the efficiency of methylene blue discoloration. *Chem. Eng. J.* **2012**, *200–202*, 433–438.
57. Miyajima, K.; Noubactep, C. Characterizing the impact of sand addition on the efficiency of granular iron for water treatment. *Chem. Eng. J.* **2015**, *262*, 891–896. [CrossRef]
58. Naseri, E.; Ndé-Tchoupé, A.I.; Mwakabona, H.T.; Nanseu-Njiki, C.P.; Noubactep, C.; Njau, K.N.; Wydra, K.D. Making Fe^0-Based filters a universal solution for safe drinking water provision. *Sustainability* **2017**, *9*, 1224. [CrossRef]
59. Phukan, M. Characterizing the Fe^0/sand system by the extent of dye discoloration. *Freib. Online Geosci.* **2015**, *40*, 1–70.
60. Varlikli, C.; Bekiari, V.; Kus, M.; Boduroglu, N.; Oner, I.; Lianos, P.; Lyberatos, G.; Icli, S. Adsorption of dyes on Sahara desert sand. *J. Hazard. Mater.* **2009**, *170*, 27–34. [CrossRef]
61. Saywell, L.G.; Cunningham, B.B. Determination of iron: Colorimetric o-phenanthroline method. *Ind. Eng. Chem. Anal. Ed.* **1937**, *9*, 67–69. [CrossRef]
62. Buck, R.P.; Rondinini, S.; Covington, A.K.; Baucke, F.G.K.; Brett, C.M.A.; Camoes, M.F.; Milton, M.J.T.; Mussini, T.; Naumann, R.; Pratt, K.W.; et al. Measurement of pH. Definition, standards, and procedures (IUPAC Recommendations 2002). *Pure Appl. Chem.* **2002**, *74*, 2169–2200. [CrossRef]
63. Noubactep, C.; Meinrath, G.; Dietrich, P.; Sauter, M.; Merkel, B. Testing the suitability of zerovalent iron materials for reactive Walls. *Environ. Chem.* **2005**, *2*, 71–76. [CrossRef]
64. Ibanez, J.G.; Gonzalez, I.; Cardenas, M.A. The effect of complex formation upon the redox potentials of metallic ions: Cyclic voltammetry experiments. *J. Chem. Educ.* **1998**, *65*, 173–175. [CrossRef]
65. Rizvi, M.A. Complexation modulated redox behavior of transition metal systems. *Rus. J. Gen. Chem.* **2015**, *85*, 959–973. [CrossRef]
66. Heimann, S. Testing granular iron for fluoride removal. *Freib. Online Geosci.* **2018**, *52*, 1–80.
67. Heimann, S.; Ndé-Tchoupé, A.I.; Hu, R.; Licha, T.; Noubactep, C. Investigating the suitability of Fe^0 packed-beds for water defluoridation. *Chemosphere* **2018**, *209*, 578–587. [CrossRef]
68. Ndé-Tchoupé, A.I.; Nanseu-Njiki, C.P.; Hu, R.; Nassi, A.; Noubactep, C.; Licha, T. Characterizing the reactivity of metallic iron for water defluoridation in batch studies. *Chemosphere* **2019**, *219*, 855–863. [CrossRef]
69. Van Genuchten, C.M.; Behrends, T.; Stipp, S.L.S.; Dideriksen, K. Achieving arsenic concentrations of <1 µg/L by Fe(0) electrolysis: The exceptional performance of magnetite. *Water Res.* **2020**, *168*, 115170.
70. Lavine, B.K.; Auslander, G.; Ritter, J. Polarographic studies of zero valent iron as a reductant for remediation of nitroaromatics in the environment. *Microchem. J.* **2001**, *70*, 69–83. [CrossRef]
71. Nesic, S. Key issues related to modelling of internal corrosion of oil and gas pipelines—A review. *Corros. Sci.* **2007**, *49*, 4308–4338. [CrossRef]

72. Lazzari, L. General aspects of corrosion. In *Encyclopedia of Hydrocarbons*; Chapter 9.1; Istituto Enciclopedia Italiana: Rome, Italy, 2008; Volume V.
73. Moraci, N.; Lelo, D.; Bilardi, S.; Calabrò, P.S. Modelling long-term hydraulic conductivity behaviour of zero valent iron column tests for permeable reactive barrier design. *Can. Geotech. J.* **2016**, *53*, 946–961. [CrossRef]
74. Santisukkasaem, U.; Das, D.B. A non-dimensional analysis of permeability loss in zero-valent iron permeable reactive barrier (PRB). *Transp. Porous Media* **2019**, *126*, 139–159. [CrossRef]
75. Magomnang, A.A.S.; Villanueva, E.P. Removal of hydrogen sulfide from biogas using dry desulfurization systems. In Proceedings of the International Conference on Agricultural, Environmental and Biological Sciences (AEBS-2014), Phuket, Thailand, 24–25 April 2014; pp. 77–80.
76. Magomnang, A.; Villanueva, E.P. Utilization of the uncoated steel wool for the removal of hydrogen sulfide from biogas. *Int. J. Min. Metall. Mech. Eng.* **2015**, *3*, 108–111.
77. Riyadi, U.; Kristanto, G.A.; Priadi, C.R. Utilization of steel wool as removal media of hydrogen sulfide in biogas. *IOP Conf. Ser. Earth Environ. Sci.* **2018**, *105*, 012026. [CrossRef]
78. Noubactep, C. The fundamental mechanism of aqueous contaminant removal by metallic iron. *Water SA* **2010**, *36*, 663–670. [CrossRef]
79. Gheju, M. Hexavalent chromium reduction with zero-valent iron (ZVI) in aquatic systems. *Water Air Soil Pollut.* **2011**, *222*, 103–148. [CrossRef]
80. Ghauch, A. Iron-based metallic systems: An excellent choice for sustainable water treatment. *Freib. Online Geosci.* **2015**, *32*, 1–80.
81. Westerhoff, P.; James, J. Nitrate removal in zero-valent iron packed columns. *Water Res.* **2003**, *37*, 1818–1830. [CrossRef]
82. Noubactep, C.; Schöner, A.; Woafo, P. Metallic iron filters for universal access to safe drinking water. *Clean Soil Air Water* **2009**, *37*, 930–937. [CrossRef]
83. Nanseu-Njiki, C.P.; Gwenzi, W.; Pengou, M.; Rahman, M.A.; Noubactep, C. Fe^0/H_2O filtration systems for decentralized safe drinking water: Where to from here? *Water* **2019**, *11*, 429. [CrossRef]
84. Hu, R.; Yang, H.; Tao, R.; Cui, X.; Xiao, M.; Konadu-Amoah, B.; Cao, V.; Lufingo, M.; Soppa-Sangue, N.P.; Ndé-Tchoupé, A.I.; et al. Metallic Iron for Environmental Remediation: Starting an Overdue Progress in knowledge. *Water* **2020**, in press.